

# Thermal analysis, X-ray and electron diffraction studies on crystalline phase transitions in solvent-treated poly(hexamethylene terephthalate)

Ming Chien Wu<sup>a</sup>, Eamor M. Woo<sup>a,\*</sup>, Taiyo Yoshioka<sup>b</sup>, Masaki Tsuji<sup>b,\*</sup>

<sup>a</sup> Department of Chemical Engineering, National Cheng Kung University, Tainan 701-01, Taiwan, ROC

<sup>b</sup> Laboratory of Chemistry of Polymeric Functionality Materials, Division of Materials Chemistry, Institute for Chemical Research, Kyoto University, Uji, Kyoto-fu 611-0011, Japan

Received 19 February 2005; received in revised form 29 April 2005; accepted 6 May 2005

Available online 11 May 2006

## Abstract

The crystal polymorphism, transformation, and morphologies in chloroform solvent-cast poly(hexamethylene terephthalate) (PHT) were examined by using differential scanning calorimetry (DSC), wide-angle X-ray diffraction (WAXD), and temperature in situ transmission electron microscopy (TEM). Solvent-induced crystallization of PHT at room temperature yielded an initial crystal of  $\gamma$ -form, as confirmed by WAXD. Upon DSC scanning, the original  $\gamma$ -form in PHT exhibited three endothermic peaks, whose origins and association were carefully analyzed. The first peak, much smaller than the other two, is in the temperature range of ca. 100–120 °C. It was found that the solvent-induced  $\gamma$ -form was transformed to  $\beta$ -form at 125 °C via a solid-to-solid transformation mechanism. In addition, WAXD showed that  $\gamma$ - and  $\beta$ -forms co-existed in the temperature range of 100–125 °C. These mixed crystal forms were further identified using TEM, and the selected-area electron diffraction (ED) patterns revealed that both  $\gamma$ - and  $\beta$ -form crystals co-existed and were packed within the same spherulite. Solid–solid transformation from the solvent-induced  $\gamma$ -form to  $\beta$ -form in PHT upon heat scanning was presented with evidence and discussed.

© 2006 Elsevier Ltd. All rights reserved.

**Keywords:** Thermal analysis; Polymorphism; Spherulites

## 1. Introduction

Polymorphism often exists in many crystalline polymers, such as syndiotactic polystyrene (sPS) [1–3,25,26], isotactic polypropylene (iPP) [4,27], and poly(butylene adipate) (PBA) [5–7]. Poly(hexamethylene terephthalate) (PHT) also possesses complex polymorphism depending on crystallization conditions. Earlier studies in the literature have shown that PHT may contain various combinations of three different crystal unit-cells, designated as  $\alpha$ ,  $\beta$  and  $\gamma$  depending on thermal and/or solvent treatments [8–10]. Recently, multiple melting characteristics and dual morphologies of PHT have also been identified [11]. In previous papers [8–10], the  $\alpha$ -form in PHT is shown to have a monoclinic unit-cell with dimensions  $a=0.910$  nm,  $b=1.756$  nm,  $c$  (chain axis) = 1.574 nm,  $\alpha=127.8^\circ$ ,  $\beta=\gamma=90^\circ$ , and is known to be favored

for crystallization under stress. The  $\beta$ - and  $\gamma$ -forms are both characterized as triclinic, with different dimension in  $b$ . The  $\beta$ -form crystal in PHT has dimensions:  $a=0.5217$  nm,  $b=0.5284$  nm,  $c$  (chain axis) = 1.5738 nm,  $\alpha=129.4^\circ$ ,  $\beta=97.6^\circ$ ,  $\gamma=95.6^\circ$ . The  $\gamma$ -form crystal cell in PHT is also triclinic and has cell dimensions and angles all equal to those for the  $\beta$ -form, except for  $b=1.0568$  nm that is exactly twice as wide as that for the  $\beta$ -form. The  $\gamma$ -form is usually obtained by solvent-induced crystallization of PHT when film-cast at room temperature [8,9]. The  $\beta$ -form can be exclusively produced in PHT by melt-crystallization only at extremely high temperatures ( $\sim 140$  °C or higher), while at lower or moderate temperatures ( $< 140$  °C), mixed crystals consisting of  $\alpha$ - and  $\beta$ -forms with various fractions in PHT are obtained [11].

Solution crystallization of macromolecules has been well discussed by Wunderlich [12]. In addition, solvent-induced crystallization has also been widely investigated in sPS [3,13–17], syndiotactic polypropylene (sPP) [18], poly(ethylene 2,6-naphthalate) (PEN) [19], poly(ethylene terephthalate) (PET) [20,21], and poly(ether ether ketone) (PEEK) [22,23]. Among these polymers, solvent-induced crystallization of sPS has been studied more extensively in recent years. sPS possesses four polymorphic crystalline forms ( $\alpha$ -,  $\beta$ -,  $\delta$ -, and

\* Corresponding authors. Tel.: +886 6275 7575; fax: +886 6234 4496.

E-mail addresses: [emwoo@mail.ncku.edu.tw](mailto:emwoo@mail.ncku.edu.tw) (E.M. Woo), [tsujimas@scl.kyoto-u.ac.jp](mailto:tsujimas@scl.kyoto-u.ac.jp) (M. Tsuji).

$\gamma$ -forms) when it is subjected to thermal and/or solution treatment. The  $\delta$ - and  $\gamma$ -forms in sPS can be induced by solvent. The  $\delta$ -form is obtained in sPS, which includes molecules of solvent in its unit cell. However, from completely desiccated sPS samples, the  $\gamma$ -form crystal is obtained [3]. Additionally, various solvents would affect the formation of crystal form. Instead of most solvents to form only the  $\delta$ -crystal of sPS, 1,1,2,2-tetrachloroethane is unique, because this solvent induces crystallization of  $\gamma$ -form in sPS [3]. Upon heating to higher temperatures, the  $\gamma$ -form crystal can be transformed to the  $\alpha$ -form one.

In this study, differential scanning calorimetry (DSC) and wide-angle X-ray diffraction (WAXD) as well as transmission electron microscopy (TEM) were utilized to identify the crystal transformation behavior and heating-induced crystal-form changes in PHT samples prepared by solution casting from chloroform at room temperature. The literature has widely reported [8–10] that the  $\gamma$ -form crystal can be produced in PHT by treatment with chloroform at room temperature and  $\beta$ -form is yielded by annealing the  $\gamma$ -form at higher temperatures; however, the mechanism of transition or thermal characteristics of these crystals has yet to be understood. With aims to extend the previous findings, this study attempted to describe the crystal-form changes as a function of temperature after initial solvent-induced crystals were generated. The crystalline morphologies of the individual PHT spherulites containing both  $\gamma$ - and  $\beta$ -forms were further characterized by ‘temperature in situ TEM’.

## 2. Experimental

### 2.1. Materials

PHT was synthesized using butyl titanate as a catalyst, according to the method described in the literature [24]. Molecular weights were determined by gel permeation chromatography (GPC) on a Waters 410 GPC system using tetrahydrofuran as the eluent at a flow rate of 1.0 mL/min. The PHT used in this study has an  $M_w = 13,800$  g/mol and a polydispersity index (PDI) of 2.0. At this molecular weight, its mechanical properties are slightly lower than those at higher molecular weights, but its thermal properties (glass transition temperature ( $T_g$ ), melting temperature ( $T_m$ ), etc.) and crystalline morphology are expected to be characteristic of a typical polymer. The thermal transition temperatures of the PHT used here may be slightly lower than those of a longer-chain PHT, but the characteristics of the crystals and multiple melting peaks were pretty much the same as those of the longer-chain PHT. The melting point (144.3 °C) and glass transition temperature (−6.7 °C) were measured by DSC.

### 2.2. Specimen preparation

Solvent-induced crystals were obtained by dissolving the synthesized PHT into chloroform to be a 4 wt% solution. The solution was dried at room temperature for 1 day, and then

the sample was dried in the vacuum oven at 40 °C for 7 days to remove the residual solvent in PHT. The solid PHT sample was directly heat-treated by DSC.

For TEM, thin films of PHT were prepared/crystallized on glass slides by casting the solution. For reinforcing the specimen, the polymer thin films were coated with vapor-deposited carbon under vacuum. In order to carry out the calibration of the diffraction camera length, gold (Au) was vapor-deposited onto some of the thin films before carbon coating. After carbon coating, a drop (a hemisphere 3–4 mm in diameter) of aqueous solution (25%) of polyacrylic acid was placed on the appropriate portion of the specimen film and hardened after drying for 1 day at room temperature. Hardened polyacrylic acid with the specimen thin film was detached from the glass plate, and then the polyacrylic acid was dissolved in water. Finally, a TEM copper grid was used to collect the specimen film floating on the water surface and then dried under ambient condition.

### 2.3. Analytical apparatus

The thermal behavior of the PHT sample was preliminarily investigated using a differential scanning calorimeter (DSC-7, Perkin–Elmer). The temperature and heat of transition indicated with the instrument were calibrated with indium and zinc standards. For determining the enthalpy of melting peaks, a dynamic heating rate of 10 °C/min was used unless otherwise indicated. During thermal treatments and DSC measurements with the DSC-7, a continuous flow of nitrogen gas into the sample-cell chamber was maintained to ensure minimal sample degradation. In addition, the DSC sample-cells were used for precisely controlling the thermal treatments of samples.

The WAXD instrument was a Shimadzu XRD-6000 (30 kV and 40 mA), and the Cu  $K_\alpha$  radiation of a wavelength of 0.1542 nm was utilized. The scattering angle,  $2\theta$ , ranged from 5 to 40° with a scanning step of 2 °/min (here,  $\theta$  is the Bragg angle). For ensuring the temperature accuracy, specimens for WAXD characterization were prepared by imposing desired thermal treatments using the DSC-7.

Morphological observation and selected-area electron diffraction (SAED) of specimens were performed with a transmission electron microscope (JEOL JEM-200CS) operated at an accelerating voltage of 200 kV. A specimen-heating holder (JEOL EM-SHH4) which has been fitted up with a homemade ‘temperature controller’ [28] was utilized to regulate the specimen temperature to be a desired temperature. The size of the selected-area aperture utilized for SAED experiments in this study was ca. 2.5  $\mu\text{m}$  in diameter on the specimen. In addition, the morphological images were taken in the conventional bright-field mode at a direct magnification of 5000 $\times$  [29,30]. All the images and SAED patterns were recorded on photographic films (Mitsubishi MEM) which were then developed with Mitsubishi Gekkol (full strength) at 20 °C for 5 min [29,31].

### 3. Results and discussion

#### 3.1. DSC and WAXD characterization of crystal transformation

It has been already mentioned that crystallization of  $\gamma$ -form could be induced by solvent at room temperature, and  $\beta$ -form is obtained after annealing the  $\gamma$ -form at the high temperatures [9]. To identify the meta-stability and phase transformation of solvent-induced PHT crystals, the solid sample of PHT was examined by DSC. Fig. 1(a) shows the DSC thermogram for the initially solvent-induced PHT sample that was scanned at 10 °C/min. The first endothermic peak (P1) at 115.5 °C designated as  $T_{m1}$  was identified. The other two endothermic peaks in this thermogram are located at 138.2 and 145.3 °C, respectively. The total endothermic heat is 64.4 J/g from the initial state to melt. However, the heat of the first peak (P1) is

only 7.2 J/g. In this thermogram, the onset and tail-end of the P1 peak are at ca. 105 and 125 °C, respectively. The initially solvent-induced PHT sample was also examined by WAXD. Fig. 1(b) shows the typical X-ray diffractogram (namely, WAXD intensity profile) of PHT crystals. The reflection peaks in the diffractogram are recognized at  $2\theta=12.1, 15.6, 17.3, 18.2, 22.2,$  and  $24.9^\circ$ . According to Palmer et al. [9], these reflection peaks are attributed to the  $\gamma$ -form.

In contrast to the heats of P2 and P3, the heat of P1 is much smaller, as shown in Fig. 1(a). Interestingly, one wonders, which crystal-form may be removed upon heating the initial  $\gamma$ -form crystal to the temperature near P1 (ca. 125 °C). Therefore, the original  $\gamma$ -form PHT samples heated to 125 °C were subjected to DSC and WAXD to observe the melting thermal characteristics and crystal diffraction peaks. For DSC measurement, the original sample was heated to 125 °C and then quenched to 0 °C. Finally, the DSC sample was scanned at 10 °C/min from 0 °C to the melt. Fig. 2(a) shows the final

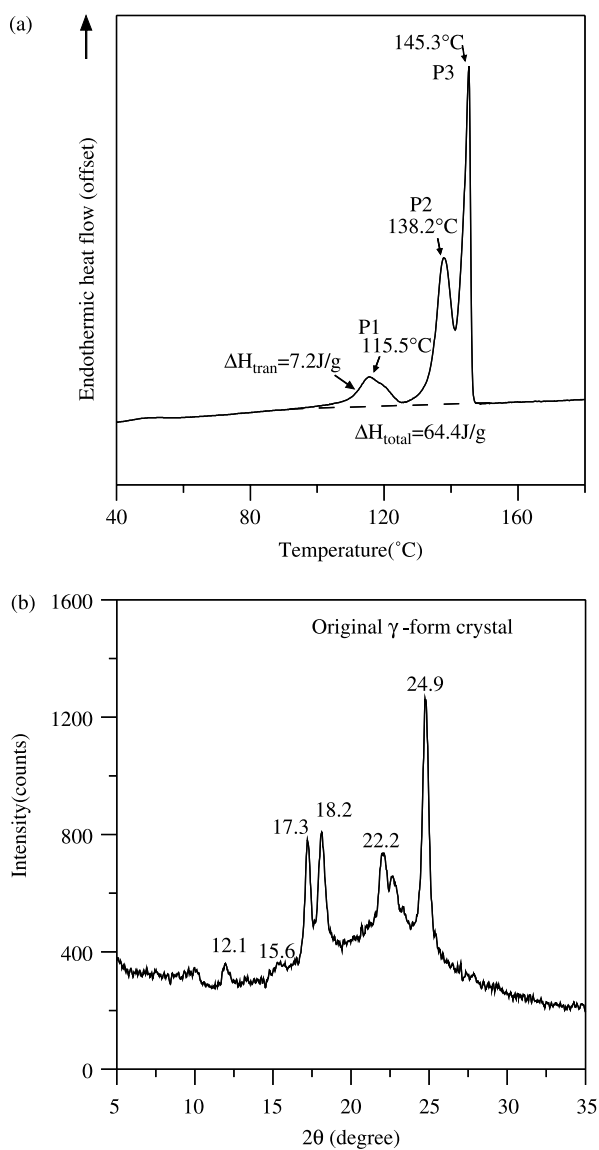


Fig. 1. (a) DSC thermogram (scanned at 10 °C/min) and (b) X-ray diffractogram for the PHT sample initially solvent-induced from chloroform at room temperature.

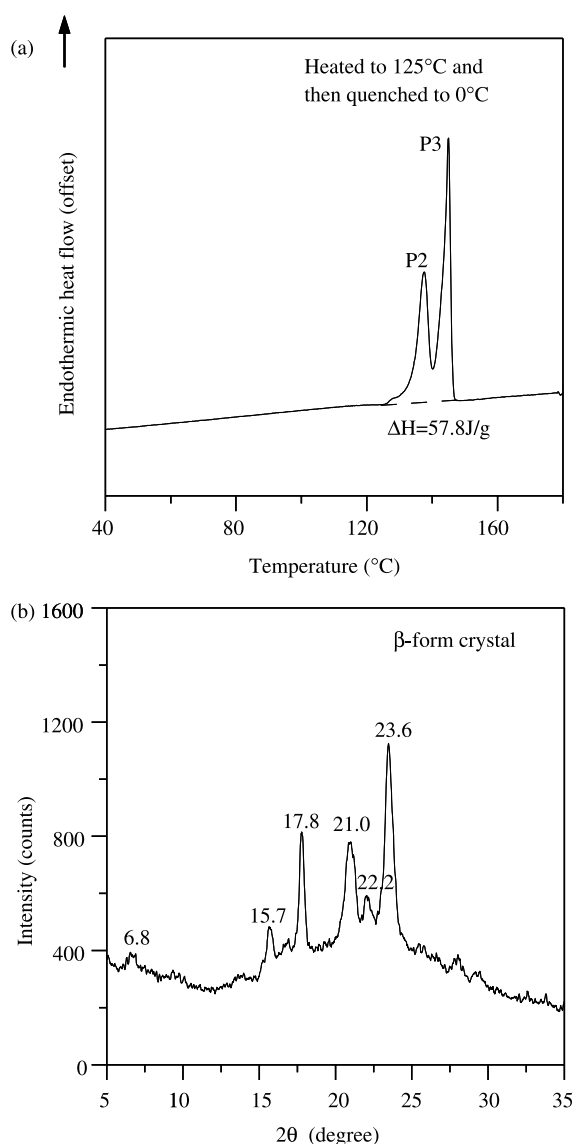


Fig. 2. (a) DSC thermogram (scanned at 10 °C/min) and (b) X-ray diffractogram for the solvent-induced PHT sample, which was further heated to 125 °C.

thermogram. In this thermogram, the *P1* peak, which is evident in Fig. 1(a), now has disappeared. In addition, the total endothermic heat reduces to 57.8 J/g. Obviously, the endothermic heat of *P1* has vanished. By comparing Fig. 2(a) with Fig. 1(a), *P2* and *P3* have no distinguishable difference in the amount of heat or temperature position. WAXD was used to examine the diffraction intensity profile of the PHT sample after the original sample was heated up to 125 °C. Fig. 2(b) shows the WAXD diffraction peaks of the heated sample. The reflection peaks are located at  $2\theta = 6.8, 15.7, 17.8, 21.0, 22.2,$  and  $23.6^\circ$  in this diffractogram. According to the earlier reports [9–11], these peaks indicate the  $\beta$  crystal form. Thus, the original solvent-induced  $\gamma$ -form crystal has been transformed to a different  $\beta$ -form by heat-treatment on solvent crystallized sample of PHT to 125 °C. The result suggests that the solvent-induced  $\gamma$ -form crystal in PHT may be readily transformed to the more stable  $\beta$ -form at temperatures between 105 and 125 °C.

The structure in thermally-induced phase transition was analyzed by performing WAXD on solvent-treated PHT samples subjected to slow heating treatment. Fig. 3 shows the WAXD intensity profiles of solvent-treated PHT samples that were subjected to step-increase of the temperature in the range of 80–125 °C. In the temperature range of 100–120 °C, the temperature interval is reduced 2 °C in order to examine the structure changes in greater details. The samples heated/annealed at lower temperatures below ca. 106 °C show characteristic  $\gamma$ -form reflection peaks. Below 106 °C, the  $\gamma$ -form reflection peak remains constant. At 108 °C or higher, the reflection peaks at  $2\theta = 15.7, 17.8, 21.0$  and  $23.6^\circ$  attributed

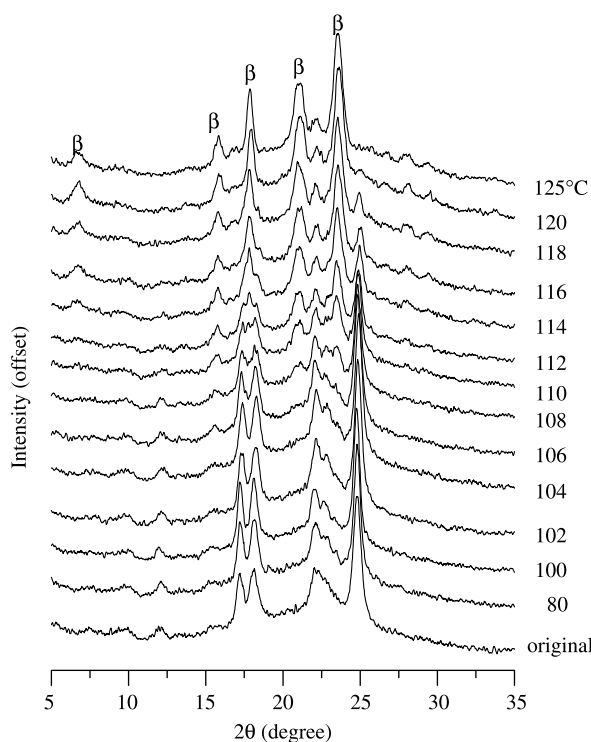


Fig. 3. X-ray diffractograms for the solvent-induced PHT samples, which were subjected to stepwise temperature increase from 80 to 125 °C.

to the  $\beta$ -form, begin to appear and increase in intensity on raising the annealing temperature. On the contrary, the  $\gamma$ -form peaks at  $2\theta = 12.1, 17.3, 18.2$  and  $24.9^\circ$  decrease in intensity with increasing annealing temperature, implying that a transition from  $\gamma$ - to  $\beta$ -form occurs. Above 120 °C, the  $\gamma$ -form diffraction peaks almost vanish.

By combining the results from DSC and X-ray, the first melting peak (*P1*) thus is related to the  $\gamma$ -form, while the two higher melting peaks are of the  $\beta$ -form. A phase transition from  $\gamma$ - to  $\beta$ -form must have taken place during heat scans. The mechanism of phase transition needs to be analyzed further using TEM and WAXD, in order to more accurately locate the crystal transition temperature.

In our earlier studies on sPS [3], it was found that the initially solvent-induced  $\gamma$ -form crystal of sPS can be transformed to  $\alpha'$ -form as the temperature is increased. At the temperature where the  $\gamma$ - to  $\alpha'$ -phase transition takes place, the crystallinity exhibits a significant increase. The increased intensity of WAXD is caused by melting of the  $\gamma$ -form of sPS and re-crystallization of the amorphous chains. In the present case, however, there is no significant change of overall intensity as a result of  $\gamma$  to  $\beta$ -crystal transformation. In the DSC thermogram of the original  $\gamma$ -form crystal, there exists no exothermic peak related to re-crystallization of the melted amorphous chains. As a result, the  $\gamma$ - to  $\beta$ -phase transition of PHT must take place via solid–solid phase transformation. Observation of morphology in the solid–solid phase transition will be evidenced by TEM in later sections.

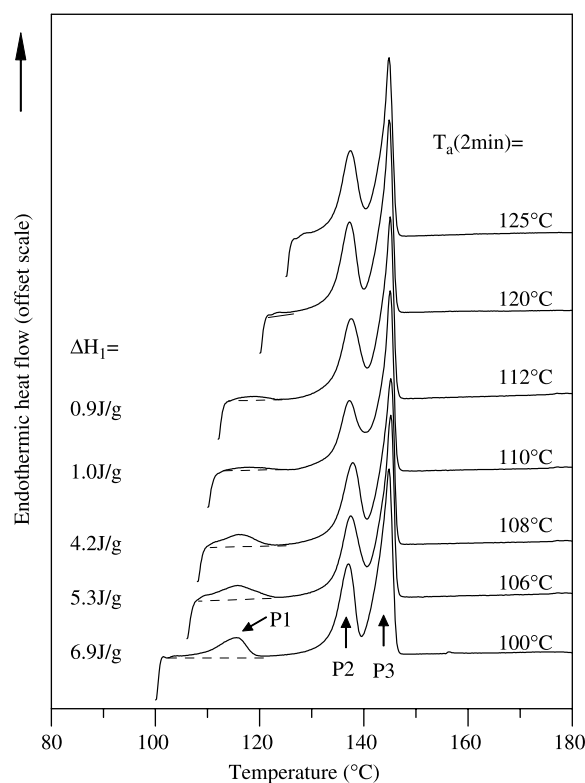


Fig. 4. DSC thermograms (scanned at 10 °C/min) for the solvent-induced PHT samples, which were heated to (a) 100 °C, (b) 106 °C, (c) 108 °C, (d) 110 °C, (e) 112 °C, (f) 120 °C, and (g) 125 °C.

As discussed above, analysis of the WAXD intensity profiles indicates that the  $\gamma$ - to  $\beta$ - phase transition occurs between 106 and 120 °C. In order to investigate the extent of transformation as a function of annealing temperature ( $T_a$ ), the originally solvent-induced  $\gamma$ -form in PHT samples was heated to specific temperatures of 100, 106, 108, 110, 112, 120 and 125 °C, respectively. After annealing at these temperatures for 2 min, the samples were then scanned in DSC to above melt. Fig. 4 shows the melting behaviors of the samples heated/annealed at these specific temperatures ( $T_a$ ). At  $T_a=100$  °C, the corresponding thermogram shows three peaks similar to those in the thermogram obtained from the original sample. The  $\Delta H_1$  related to the endothermic heat of  $P_1$  is 6.9 J/g. Further increase of annealing temperature was imposed on the samples. The reduced endothermic heat of  $P_1$  was present. At  $T_a=125$  °C, however,  $P_1$  does not exist in the thermogram. As for

$T_a=120$  °C, the heat of  $P_1$  is so small that it is difficult to calculate the endothermic heat. However, a very small  $P_1$  indeed existed in the thermogram of  $T_a=120$  °C. Corresponding to the WXAD result, the smaller heat of  $P_1$  represents that more fraction of  $\gamma$ -form transforms to  $\beta$ -form.

The effect of annealing time ( $t_a$ ) on the phase transition was also explored. The original  $\gamma$ -form PHT samples were heated to 100 °C and annealed for 2 or 960 min. Fig. 5 shows the results of (a) DSC and (b) WAXD. In Fig. 5(a), both DSC thermograms have three endothermic peaks. However, when  $t_a=960$  min, the  $P_1$  and  $P_2$  shift to higher temperatures, and the enthalpy associated to  $P_1$  is reduced. The corresponding X-ray diffractograms are shown in Fig. 5(b). For  $t_a=960$  min,

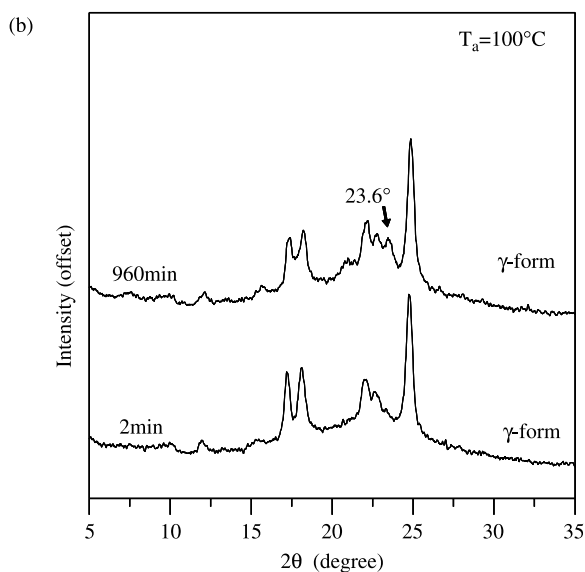
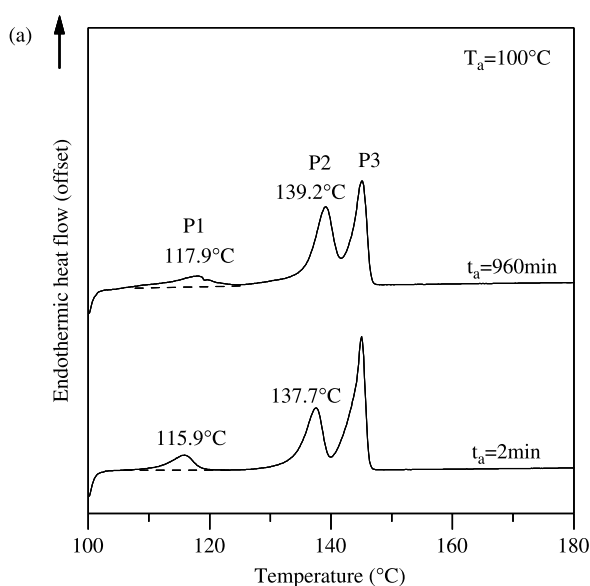


Fig. 5. (a) DSC thermograms (scanned at 10 °C/min) and (b) X-ray diffractograms for the solvent-induced PHT samples, which were heated to 100 °C and then annealed for 2 or 960 min.

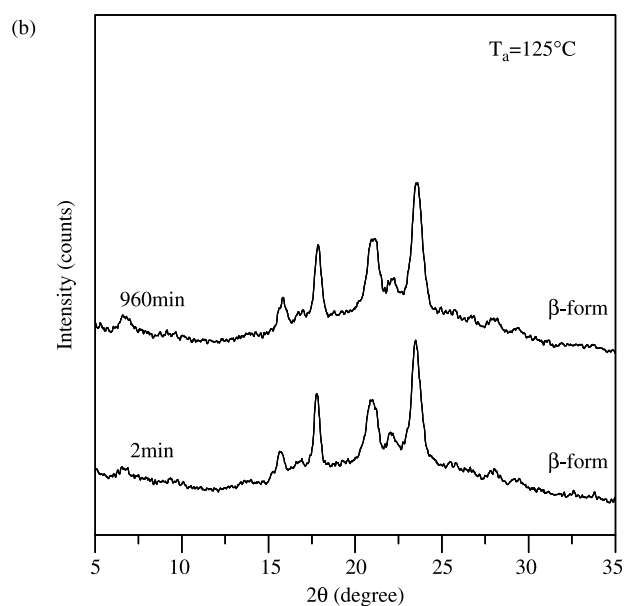
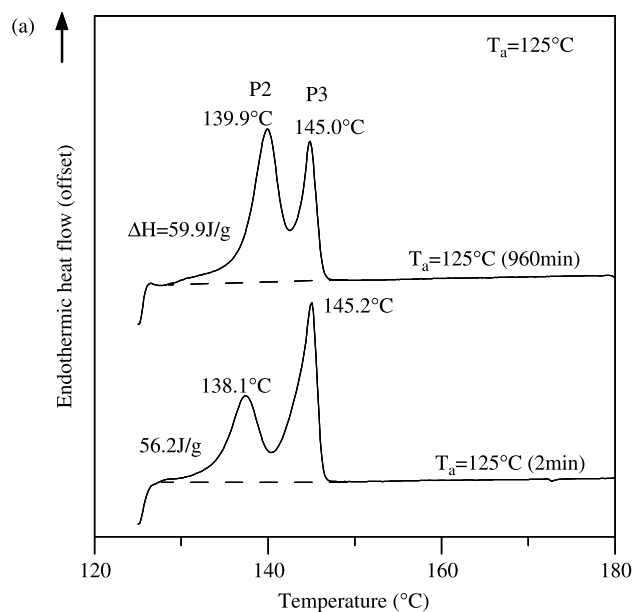


Fig. 6. (a) DSC thermograms (scanned at 10 °C/min) and (b) X-ray diffractograms for the solvent-induced PHT samples, which were heated to 125 °C and then annealed for 2 or 960 min.

all the reflection peaks are attributed to the  $\gamma$ -form except for the small peak at  $2\theta=23.6^\circ$ . Consequently, very long annealing times are needed to induce a small phase transition of  $\gamma$ -form PHT at  $T_a=100^\circ\text{C}$ .

Similarly, annealing treatments were applied to the original  $\gamma$ -form samples at  $125^\circ\text{C}$ . The DSC and WAXD results are shown in Fig. 6(a) and (b). Both DSC thermograms in Fig. 6(a) show a similar total heat. However, for the longer annealing

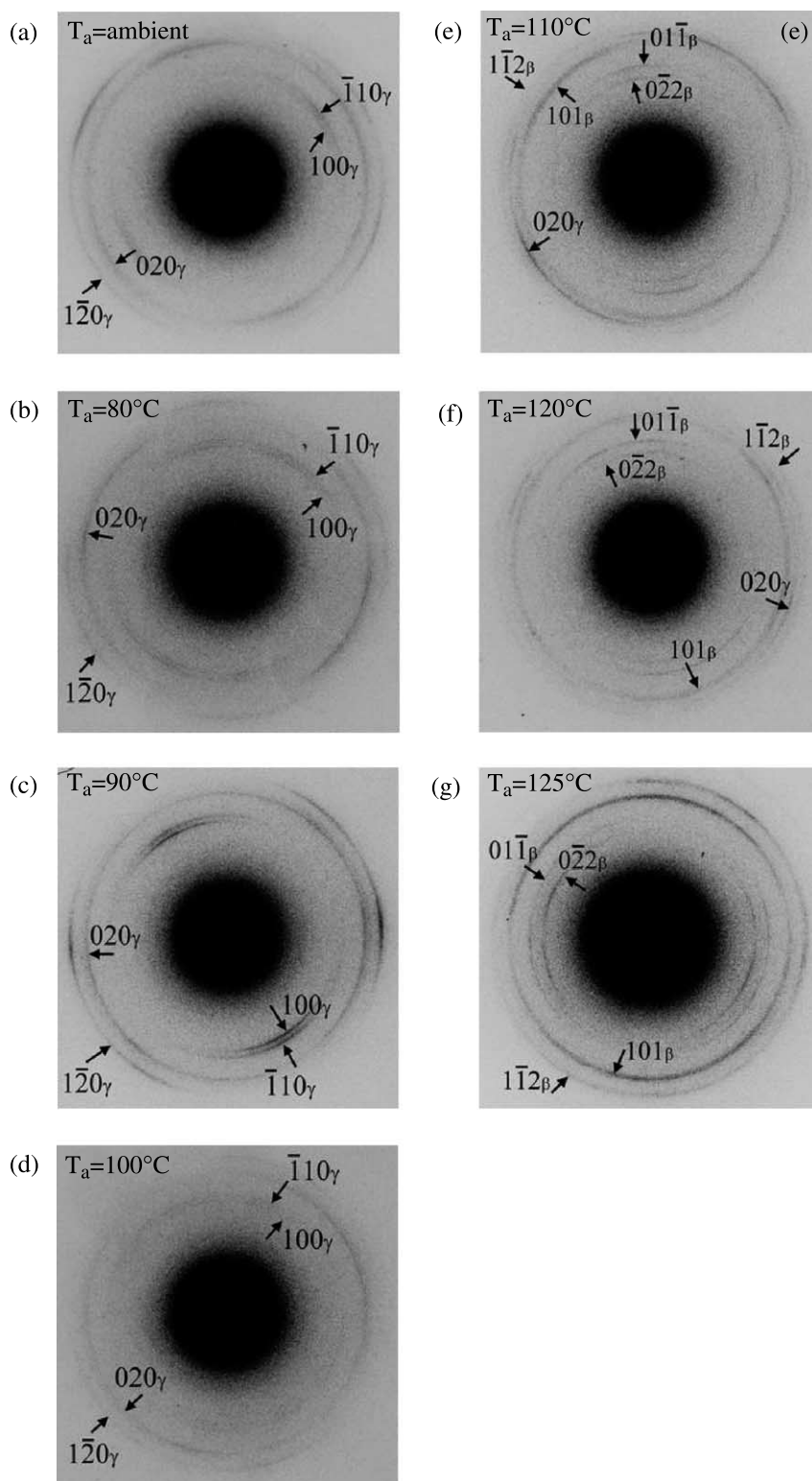


Fig. 7. Temperature series of SAED patterns (reversed contrast) obtained from a same thin film specimen of solvent-induced PHT, which were recorded at (a) room temperature, (b)  $80^\circ\text{C}$ , (c)  $90^\circ\text{C}$ , (d)  $100^\circ\text{C}$ , (e)  $110^\circ\text{C}$ , (f)  $120^\circ\text{C}$ , and (g)  $125^\circ\text{C}$ . The size of the selected-area aperture utilized for SAED experiments was ca.  $2.5\ \mu\text{m}$  in diameter on the specimen.

Table 1  
 $d$ -Spacings of WAXD and SAED and reflection indices for the  $\gamma$ - and  $\beta$ -form crystals of poly(hexamethylene terephthalate) (PHT)

X-ray diffraction peak at $2\theta$ (°)	$d_{\text{obs-WAXD}}$ (nm)	$d_{\text{obs-SAED}}$ (nm)	$hkl$
$\gamma$ -Form			
12.1	0.732	–	
15.6	0.568	–	
17.3	0.513	0.505	100
18.2	0.487	0.480	$\bar{1}10$
22.2	0.400	0.396	020
24.9	0.358	0.356	$1\bar{2}0$
$\beta$ -Form			
6.8	1.300	–	
15.7	0.564	0.544	$0\bar{2}2$
17.8	0.498	0.484	$01\bar{1}$
21.0	0.423	0.413	101
23.6	0.377	0.371	$1\bar{1}2$

times, the heat of fusion of  $P2$  increases and  $P2$  shifts to a higher temperature, suggesting that the crystals probably thicken during long annealing times. The X-ray diffraction intensities in Fig. 6(b) show that the  $\beta$ -form crystal is not affected after annealing for  $t_a=960$  min at  $T_a=125$  °C.

### 3.2. In situ TEM on phase transition in PHT

The thin film specimen of solvent-induced PHT prepared by the method described in Section 2 was introduced into the TEM column with the specimen-heating holder. The specimen was heated from room temperature up to 125 °C, and the SAED patterns of PHT crystals were obtained at different temperatures from a same thin film specimen. Fig. 7(a)–(g) displays a temperature series of SAED patterns (reversed contrast) from an area about 2.5  $\mu\text{m}$  in diameter. Fig. 7(a) shows the SAED pattern of the original solvent-induced PHT crystal recorded before heating. The  $d$ -spacing values of the observed arc-shaped reflections are 0.513, 0.487, 0.400 and 0.358 nm, which correspond to  $100_\gamma$ ,  $\bar{1}10_\gamma$ ,  $020_\gamma$ , and  $1\bar{2}0_\gamma$  reflections, respectively, as indicated in Fig. 7(a). Here, the subscript,  $\gamma$ , represents the reflection of  $\gamma$ -form. Meanwhile, tabulated values for comparing SAED and WAXD results may help. Table 1 shows the comparison of values of  $d$ -spacing for the  $\gamma$ -form crystal, which were obtained by the WAXD and SAED

analyses. The results indicate that values of  $d$ -spacing obtained by SAED are almost same as those measured by WAXD; however, the WAXD peaks at  $2\theta=12.1$  and  $15.6^\circ$  are so weak that the corresponding reflections were not recognized in the SAED pattern. Subsequently, the thin film was heated in the specimen holder to 80 °C. Fig. 7(b) is the SAED pattern obtained from the specimen treated at 80 °C. Overall, below 100 °C, the SAED patterns were similar to the original sample (Fig. 7(a)) in agreement also with the data in Fig. 3 shown earlier. Above 100 °C, more dramatic changes in the crystal forms are seen. At 110 °C, the  $100_\gamma$ ,  $\bar{1}10_\gamma$ , and  $1\bar{2}0_\gamma$  reflections disappear in the SAED pattern, whereas  $0\bar{2}2_\beta$ ,  $01\bar{1}_\beta$ ,  $101_\beta$ , and  $1\bar{1}2_\beta$  appear. At 120 °C, only a weak  $020_\gamma$  reflection still exists, but it completely disappears at 125 °C, leaving only four  $\beta$ -form reflections. These  $\beta$ -form reflections at 125 °C have  $d$ -spacings of 0.564, 0.498, 0.423, and 0.377 nm, which correspond to  $0\bar{2}2_\beta$ ,  $01\bar{1}_\beta$ ,  $101_\beta$ , and  $1\bar{1}2_\beta$ , respectively. Again, the bottom portion of Table 1 lists and compares the values of  $d$ -spacing of  $\beta$ -form reflections observed by WAXD and SAED analyses. In addition, it is worth mentioning that experimentally all SAED patterns were obtained by focusing within the same one spherulite. The result suggests that the  $\gamma$ - and  $\beta$ -form crystals, therefore, co-exist within a single spherulite in the solvent-treated PHT annealed in the temperature range of ca. 110–120 °C.

A temperature series (ambient to 125 °C) of in situ TEM images were produced by focusing on the spherulites in a same thin film specimen of solvent-induced PHT. Various positions of the thin film specimen were observed in order to avoid looking at accidentally damaged spherulites. The specimens were heated to higher temperatures by using the in situ heating holder in TEM. The morphological images of the spherulites were recorded in series at ambient, 80, 90, 100, 110, 120, and 125 °C, respectively. Finally, Fig. 8 shows the TEM images for two specimens of the solvent-induced PHT at (a) ambient, and (b) 125 °C. As all the temperature series images (ambient, 80, 90, 100, 110, 120, and 125 °C) are similar; thus, only two representative TEM images are shown here. In comparison with the as-prepared PHT sample, the spherulites heated to temperatures ranging from ambient to 125 °C remain unchanged (for brevity, similarity in the series are not all shown). Comparatively speaking, the temperature series TEM

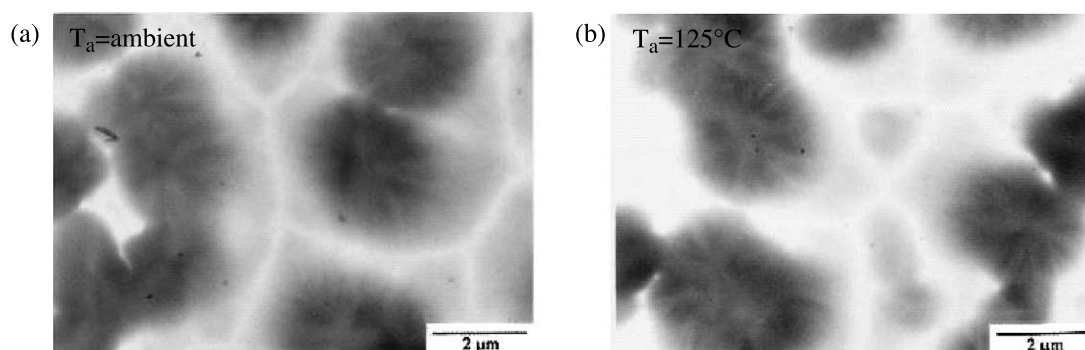


Fig. 8. Temperature in situ TEM images showing spherulitic morphology in a same thin film specimen of solvent-induced PHT, taken in conventional bright-field imaging mode at (a) ambient temperature, and (b) 125 °C.

images between ambient and 125 °C are all similar without indication of transition into liquid molten state. As a result, it can be proposed that the  $\gamma$ - to  $\beta$ -phase transition of the solvent-induced PHT crystals takes place in the solid state without going through melting.

#### 4. Conclusion

The DSC analysis on the PHT samples solvent-cast from chloroform at room temperature displays three endothermic peaks, indicating a crystal polymorphism and/or crystal–crystal transformation. The WAXD results suggest that the initial solvent-cast PHT film is only of the  $\gamma$ -form crystal. Upon annealing at 125 °C, however, a new  $\beta$ -form crystal is formed, which exhibits two melting peaks (*P2* and *P3*) upon DSC scanning. The first melting peak (*P1*) is related to the  $\gamma$ -form. It implies that phase transition from  $\gamma$ - to  $\beta$ -form must have taken place during DSC heat scans. WAXD data show that only the  $\gamma$ -crystal exists in the original solvent-cast PHT, but both  $\gamma$  and  $\beta$  crystal-forms can co-exist in various fractions in solvent-cast PHT samples further heated/annealed between 106 and 120 °C. When annealed at 125 °C and above, PHT exhibits only the  $\beta$ -form crystal, suggesting a phase transition.

Further evidence of the crystal phase transition and its mechanism was obtained by performing in situ TEM characterization. In the SAED patterns obtained below 100 °C, only the  $\gamma$ -form is evident. Between 110 and 120 °C, both  $\gamma$ - and  $\beta$ -forms co-exist within the same spherulite in PHT. This feature, combined with the fact that the spherulite remains unchanged in state, indicates that the  $\gamma$ -to- $\beta$  transition of the solvent-induced crystal in PHT is a solid–solid transformation.

#### Acknowledgements

The authors acknowledge the research grants from Taiwan's National Science Council (#NSC92-2216-E006-015). In addition, M.-C. Wu, a PhD candidate student at National Cheng Kung University, Taiwan, appreciates the sponsorship by Interchange Association (Japan) to spend summer internship at the Institute for Chemical Research, Kyoto University, Japan, under guidance of Prof. M. Tsuji. The TEM work in this study was supported by a Grant-in-Aid for Scientific Research (c) (2), No. 16550174, from Japan Society for the Promotion of Sciences (JSPS), to which M. Tsuji wishes to

express his gratitude. Lastly but most importantly, our gratitude is also due to the Guest Editors, who kindly invited and gave a privilege to us to contribute to the special issue honoring Professor David Bassett.

#### References

- [1] Guerra G, Vitagliano VM, De Rosa C, Petraccone V, Corradini P. *Macromolecules* 1990;23:1539.
- [2] Woo EM, Sun YS, Yang CP. *Prog Polym Sci* 2001;26:945.
- [3] Sun YS, Woo EM, Wu MC, Ho RM. *Polymer* 2003;44:5293.
- [4] Bruckner S, Meille SV, Petraccone V, Pirozzi B. *Prog Polym Sci* 1991;16:361.
- [5] Minke R, Blackwell JJ. *Macromol Sci Phys* 1979;B16:407.
- [6] Minke R, Blackwell JJ. *Macromol Sci Phys* 1980;B18:233.
- [7] Gan Z, Abe H, Doi Y. *Macromol Chem Phys* 2002;203:2369.
- [8] Hall IH, Ibrahim BA. *Polymer* 1982;23:805.
- [9] Palmer A, Poulin-Dandurand S, Revol JF, Brisse F. *Eur Polym J* 1984;20:783.
- [10] Brisse F, Palmer A, Moss B, Dorset D, Roughead WA, Miller DP. *Eur Polym J* 1984;20:791.
- [11] Woo EM, Wu PL, Chiang CP, Liu HL. *Macromol Rapid Commun* 2004;25:942.
- [12] Wunderlich B. *Macromolecular physics*, vol. 2. New York: Academic Press; 1976 p. 197.
- [13] Sun YS, Woo EM, Wu MC, Ho RM. *Macromolecules* 2003;36:8415.
- [14] Gupper A, Andrew CKL, Kazarian SG. *Macromolecules* 2004;37:6498.
- [15] Yoshioka A, Tashiro K. *Polymer* 2003;44:6681.
- [16] Yoshioka A, Tashiro K. *Macromolecules* 2002;35:410.
- [17] Ray B, Elhasri S, Thierry A, Marie P, Guenet JM. *Macromolecules* 2002;35:9730.
- [18] Gorrasi G, Guadagno L, Vittoria V. *Colloid Polym Sci* 2003;281:469.
- [19] Kim SJ, Nam JY, Lee YM, Im SS. *Polymer* 1999;40:5623.
- [20] Im SS, Lee HS. *J Appl Polym Sci* 1989;37:1801.
- [21] Ouyang H, Lee WH, Shiue ST, Lin TL. *J Polym Sci: Part B* 2002;40:1444.
- [22] Zhang MQ, Ning KJ, Li TQ, Zeng HM. *J Appl Polym Sci* 1999;74:3376.
- [23] Cornelis H, Kander RG, Martin JP. *Polymer* 1996;37:4573.
- [24] Gilbert M, Hybart FJ. *Polymer* 1972;13:327.
- [25] Tsuji M, Okihara T, Tosaka M, Kawaguchi A, Katayama K. *MSA Bull* 1993;23:57.
- [26] Tosaka M, Tsuji M, Kohjiya S, Cartier L, Lotz B. *Macromolecules* 1999;32:4905.
- [27] Tosaka M, Endo Y, Murakami S, Tsuji M, Kohjiya S. *Sen'i Gakkaishi* 2001;57:207.
- [28] Shimizu T, Tsuji M, Kohjiya S. *Sen'i Gakkaishi* 2001;57:137.
- [29] Tsuji M. In: Sir Allen G, Bevington JC, editors. *Comprehensive polymer science*. *Comprehensive polymer science*, vol. 1. Oxford: Pergamon Press; 1989. p. 785–840 [Vol. Eds.: Booth C. and Price C., chapter 34].
- [30] Tsuji M, Kohjiya S. *Prog Polym Sci* 1995;20:259.
- [31] Tsuji M, Fujita M. *Encyclopedia of materials: science and technology*. Amsterdam: Elsevier Science; 2001 p. 7654–64.